RSC Advances

PAPER

Cite this: *RSC Adv.*, 2014, **4**, 51688

Biodiesel synthesis over the $CaO–ZrO_2$ solid base catalyst prepared by a urea–nitrate combustion method

Shengfei Xia, Xiaoming Guo,* Dongsen Mao, Zhangping Shi, Guisheng Wu and Guanzhong Lu

$CaO–ZrO_2$ solid base catalysts with Ca/Zr ratios varying from 4/6 to 9/1 were prepared *via* a urea–nitrate combustion method and used in the transesterification of soybean oil with methanol to produce biodiesel. The catalysts were characterized using N_2 adsorption, XRD, SEM and CO_2-TPD techniques, and tested for biodiesel synthesis. The results show that a new phase of $CaZrO_3$ has been formed for the investigated $CaO–ZrO_2$ catalysts. With the increase in Ca/Zr molar ratio, the total basic sites over the catalyst increase and a maximum is obtained over the $CaO–ZrO_2$ catalyst with a Ca/Zr ratio of 8/2. A similar variation trend of biodiesel yield is observed, suggesting that the catalytic activity correlates well with the total basic sites on the catalyst surface. Furthermore, the turnover frequency (TOF) has been calculated for various $CaO–ZrO_2$ catalysts and the result revealed that the catalytic activity also depends on the strength of basic sites. The urea–nitrate combustion method was demonstrated to be a simple, fast and effective method for the preparation of $CaO–ZrO_2$ solid base catalysts, which could be effectively applied for biodiesel synthesis.

Received 4th August 2014
Accepted 6th October 2014

DOI: 10.1039/c4ra11362d

www.rsc.org/advances

1. Introduction

Due to the diminishing fossil fuel resources and the soaring global energy demands, the development of renewable energy sources has gained increasing attention in recent years. Biodiesel, typically consisting of fatty acid methyl ester (FAME), can be produced by a transesterification of vegetable oil or animal fat with methanol in the presence of a suitable catalyst. Because of its renewable nature, environmentally friendly properties as well superior performance during the combustion process, biodiesel is a promising alternative to the traditional fossil diesel fuel.[1–5]

Two kinds of catalysts, homogeneous and heterogeneous catalysts, have been used for the transesterification reaction. Although homogenous catalysts allow transesterification to be performed in a shorter reaction time under moderate operating conditions, the catalyst separation and biodiesel purification steps will produce a large amount of waste water leading to an increase in production cost and environmental pollution.[6–9] Therefore, the research has been directed towards the development of heterogeneous catalysts. A serial of solid acid catalysts based on sulfated metal oxides had been prepared by Dimian *et al.* and used for the fatty acid esterification.[10,11] However, for the transesterification reaction, the performances of solid acid catalysts are still inferior compared with the solid base catalysts.[12] For this reason, a variety of heterogeneous solid base catalysts have been examined in transesterification reactions for biodiesel synthesis.[12–16]

Among these solid base catalysts, CaO is the best-known and most intensively investigated system for its economy and reactivity.[17–19] However, some reports indicated that pure CaO catalyst was sensitive to atmospheric CO_2, and it slightly dissolved in methanol during the transesterification process.[17,20,21] In addition to that, the mechanical strength of CaO particle is weak, which leads to the collapse of catalyst in a reactor and limits its industrial application.[21,22] In order to improve the stability of CaO catalyst, a strategy of combining CaO with other metal oxides is adopted.[23,24] Recently, the mixed oxide catalysts of Ca and Zr were popularly used for the transesterification reactions, and an excellent catalytic performance could be achieved.[25–29]

The traditional methods, such as co-precipitation,[25–27] impregnation,[26,28] physical mixing[26] and sol–gel,[29] have been employed to prepare $CaO–ZrO_2$ mixed oxide catalysts. However, most of these methods suffer from either the procedures of complexity and time-consuming or the requirement of expensive starting materials. Especially, a calcination process with high temperature of 700–900 °C and long-time is indispensable, which will result in a phenomenon of catalyst agglomeration and further diminish the catalytic activity. Compared with these traditional methods, combustion synthesis, based on the principles of the propellant chemistry, has been extensively used to

Research Institute of Applied Catalysis, School of Chemical and Environmental Engineering, Shanghai Institute of Technology, Shanghai 201418, P. R. China. E-mail: guoxiaoming@sit.edu.cn; Fax: +86-21-60873301; Tel: +86-21-60873301

prepare mixed oxide catalysts for its advantages of applying inexpensive raw materials, maintaining a relatively simple and fast preparation process, and achieving fine powders with high homogeneity.[30–33] To our best knowledge, there is no article regarding the synthesis of CaO–ZrO_2 solid base catalyst using the combustion method.

In this work, CaO–ZrO_2 solid base catalysts with the molar ratio ranged from 4/6 to 9/1 for the transesterification of soybean oil were prepared by urea–nitrate combustion method without a further high temperature and longtime calcinations step. The combustion reactions are analyzed in terms of propellant chemistry and the combustion behaviors are detected. The prepared CaO–ZrO_2 catalysts have been examined by various characterization techniques. The effects of Ca/Zr molar ratio on the physicochemical property and catalytic activity were emphasized. Furthermore, the relationship between the basicity and catalytic activity of the catalysts for transesterification were discussed in detail.

2. Experimental

2.1. Catalyst preparation

A serial of CaO–ZrO_2 catalysts with different Ca/Zr molar ratios were prepared using urea–nitrate combustion method. Firstly, $Ca(NO_3)_2 \cdot 4H_2O$ and $Zr(NO_3)_4 \cdot 5H_2O$ (AR grade, Shanghai Chemical Reagent Corporation, Shanghai, China) were mixed with a small quantity of deionized water in a basin. The resulting mixture was stirred and heated at 80 °C until a transparent aqueous solution was obtained. Then the required amount of urea was slowly added to the metal nitrate solution under constant stirring. Afterward, the basin was introduced in an open muffle furnace preheated at 500 °C. The solution started boiling and frothing, and in a short time ignited spontaneously with rapid evolution of a large quantity of gases, yielding a foamy, voluminous powder. The maximum temperature reached during the combustion process was measured with a chrome–alumel (K type) thermocouple whose hot junction was placed right over the mouth of the basin. The synthesized catalysts are denoted as C_xZ_y, where x and y represent the atomic concentration of Ca and Zr, respectively. In addition, in order to make a comparison, a typical CaO–ZrO_2 catalyst with Ca/Zr molar ratio of 8/2 was prepared by the conventional carbonate co-precipitation method described previously.[25]

2.2. Catalyst characterization

The dried semi-solid gel obtained by heating the precursor at 80 °C for 8 hours was collected prior to combustion reaction for a thermal analysis measurement. The thermal gravimetric and differential scanning calorimetry (TG-DSC) profiles were recorded on a thermal analyzer (STA 449-F3, NETZSCH) at a heating rate of 5 °C min^{-1} under a continuous flow of air.

X-ray diffraction (XRD) patterns were recorded with a PANalytical X'Pert diffractometer operating with Ni β-filtered Cu Kα radiation at 40 kV and 40 mA. Two theta angles ranged from 10 to 70° with a speed of 6° per minute.

Full nitrogen adsorption/desorption isotherms at −196 °C were obtained after outgassing the sample under vacuum at 200 °C for 4 h, using a Micromeritics ASAP2020 M + C adsorption apparatus. Specific surface area (S_{BET}) was calculated using a value of 0.162 nm^2 for the cross-sectional area of the nitrogen molecule.

The surface morphology was observed by the scanning electronic microscopy (SEM, S-3400N, Hitachi). The samples were coated with gold using a sputter coater.

The basicity of the catalysts was measured by CO_2 temperature-programmed desorption (CO_2-TPD). Prior to the adsorption of CO_2, the catalysts were heated at 600 °C for 60 min to clean the surface from moisture and other adsorbed gases. After cooling to room temperature, the catalyst was saturated with CO_2 at 50 °C for 60 min, and then flushed with He flow to remove any physisorbed molecules. Afterward, the TPD experiment was started with a heating rate of 5 °C min^{-1} under He flow, and the desorbed CO_2 was detected by a thermal conductivity detector (TCD). The amount of the desorbed CO_2 was quantified by comparing the integrated area of the TPD curves to the peak area of the injected CO_2 calibration pulse.

^{1}H nuclear magnetic resonance (^{1}H NMR) spectra were recorded on a Bruker AVANCE-III 500 spectrometer with tetramethylsilane as the internal reference using $CDCl_3$ as a solvent in all cases.

2.3. Transesterification reaction

The transesterification reactions (Scheme 1) were carried out in a 250 ml three-neck round bottom flask, equipped with a water-cooled reflux condenser and a magnetic stirrer. The reaction procedure was as follows: first, the catalyst was dispersed in methanol under a stirring rate of 500 rpm. Then, the soybean oil (purchased from Shanghai Jiali Oil Plant, acid value < 0.2 mg KOH per gram) was added into the mixture and heated to a controlled temperature of 65 °C by an oil bath. To monitor the progress of reaction, a sample (0.5 ml) was withdrawn by drip tube each time from the reaction mixture at an interval of 0.5 h, and then centrifuged to get phase separation. Before the analysis of FAME yield, the upper layer was washed three times with brine to ensure complete removal of glycerol and alkali, and finally dried over anhydrous $MgSO_4$.

2.4. Product analysis

^{1}H NMR technique was employed to estimate the yield of FAME using the following formula[34]

$$Y\% = \frac{2A_1}{3A_2} \times 100$$

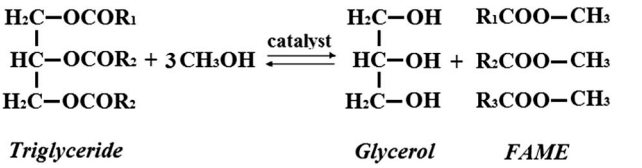

Scheme 1 Transesterification of triglycerides with methanol.

where A_1 and A_2 are the areas of ^{1}H NMR peaks corresponding to the methoxy protons (CH_3O–) in the methyl ester at chemical shifts of 3.68 ppm (singlet peak) and methylene protons (–CH_2–) of all triglycerides at chemical shifts of 2.30 ppm (triplet peak), respectively. The factors 3 and 2 derive from the number of attached protons at the methoxy and methylene carbons.

3. Results and discussion

3.1. Combustion reaction analysis and combustion behavior

For urea–nitrate combustion, primarily N_2, CO_2, and H_2O are evolved as the gaseous products.[35,36] Thus, the combustion reactions in the present paper can be represented as follows:

$$x\mathrm{Ca(NO_3)_2{\cdot}4H_2O} + y\mathrm{Zr(NO_3)_4{\cdot}5H_2O} + m\mathrm{CO(NH_2)_2} + (3m - 5x - 10y)/2\mathrm{O_2} \rightarrow (\mathrm{CaO})_x(\mathrm{ZrO_2})_y + (x + 2y + m)\mathrm{N_2} + m\mathrm{CO_2} + (4x + 5y + 2m)\mathrm{H_2O}$$

According to the principle of propellant chemistry,[37] for stoichiometric redox reaction between a fuel and an oxidizer, the ratio of the net oxidizing valence of the metal nitrate to the net reducing valence of the fuel should be unity. In this case, 1 mol C_xZ_y stoichiometrically requires $(5x + 10y)/3$ mol urea (*i.e.* $m = (5x + 10y)/3$) without the necessity of getting oxygen from atmosphere. When the urea amount is smaller than that of stoichiometry, the combustion reaction is called a fuel-deficient reaction. For this case, the value of $(3m - 5x - 10y)$ would be negative, suggesting that O_2 would be evolved in the products. However, when the urea amount is larger than that of stoichiometry, corresponding to a fuel-rich reaction, atmospheric O_2 had been involved ensuring the complete combustion of urea.

It is well known that the fuel content is one of the most important parameters in combustion synthesis. To investigate the influence of fuel amount on the combustion reaction, the urea amount of 50% (fuel-deficient), 100% (stoichiometric) and 150% (fuel-rich) of stoichiometric amount were employed for the synthesis of the C_xZ_y sample. It was experimentally observed that the combustion appears in a smoldering manner for the fuel-deficient precursor. On the other hand, the stoichiometric and fuel-rich precursor exhibited incandescent flame growing after auto-ignition, and the autoignition of the latter was found to be more violent compared to that of the former. This means that the combustion intensity enhances with the increase in urea amount, and similar result had been reported in the literature.[32,38] Hereinafter, 150% of stoichiometric amount urea was adopted to achieve a full decomposition of nitrate, urea and possible carbon residues produced in the combustion process.

The highest flame temperatures measured with the thermocouple appear at 1000–1100 °C for the samples with different Ca/Zr ratio, and the duration of combustion is about one minute. Certainly, the highest flame temperature also can be thermaldynamically estimated under the assumption that the combustion is an adiabatic process. Because of heat losses, incomplete combustion, and heating of air, it can be conceived that the measured flame temperatures were lower than the theoretical adiabatic flame temperatures.[39]

The combustion behavior of the dried gel collected prior to decomposition was also monitored by TG-DSC. A typical TG-DSC plot for the C_8Z_2 sample is shown in Fig. 1. It can be seen that a weight loss of about 4% with a concurrent endothermic peak locates at 30–160 °C, which is attributed to the vaporization of physically absorbed water and the dehydration reaction of gels. Another weight loss stage occurs at 160–240 °C. It is associated with an endothermic peak centered at 210 °C and can be assigned to the decomposition of a small amount zirconium nitrate. In the temperature range of 240–550 °C, a huge weight loss accompanied by a marked exothermic effect clearly indicates the combustion reaction between urea and NO_3^-. At temperature above 600 °C, the weight loss is negligible, and this indicates that the decomposition of precursor completed before 600 °C. The total weight loss determined for the production of C_8Z_2 was 77.3%, and it was approximate to the theoretical value of 81.5%. These results of thermoanalysis confirm that Ca–Zr complex oxide can be synthesized effectively during the combustion reaction although the duration of combustion is rather short, requiring no further calcinations at such a high temperature of 800 °C, which is employed necessarily in the preparation of Ca-based solid base with traditional methods.[40]

3.2. Structure and texture of the catalysts

The XRD patterns of CaO–ZrO_2 catalysts with varied Ca/Zr molar ratios were shown in Fig. 2(A). The diffraction peaks at 2θ of 32.2°, 37.3°, and 53.9° are ascribed to CaO phase (JCPDS 070-4068). In the case of C_4Z_6 and C_5Z_5, no diffraction lines of CaO are detected, suggesting that CaO is incorporated into ZrO_2 lattice to form homogenous CaO–ZrO_2 solid solution.[25,26,41] As the Ca/Zr ratio increase to 6/4, the diffraction peaks of CaO appear, and the relative intensity of the peaks increase with a further increase in the amount of Ca. This indicates that excessive Ca^{2+} cannot enter the solid solution and exist in the free CaO. The characteristic diffraction peaks of $CaZrO_3$ (JCPDS 076-2401) corresponding to the crystallized solid solution of CaO–ZrO_2, were observed at 2θ of 22.1°, 31.5°, and 45.1° for all investigated samples. With the increase in the Ca/Zr ratio, the

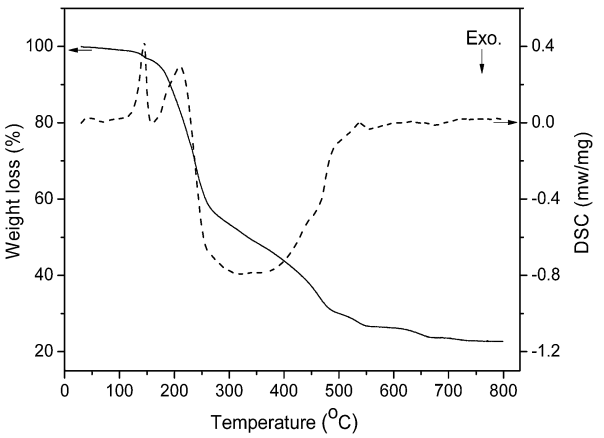

Fig. 1 TG and DSC profiles for the dried gel of C_8Z_2 sample.

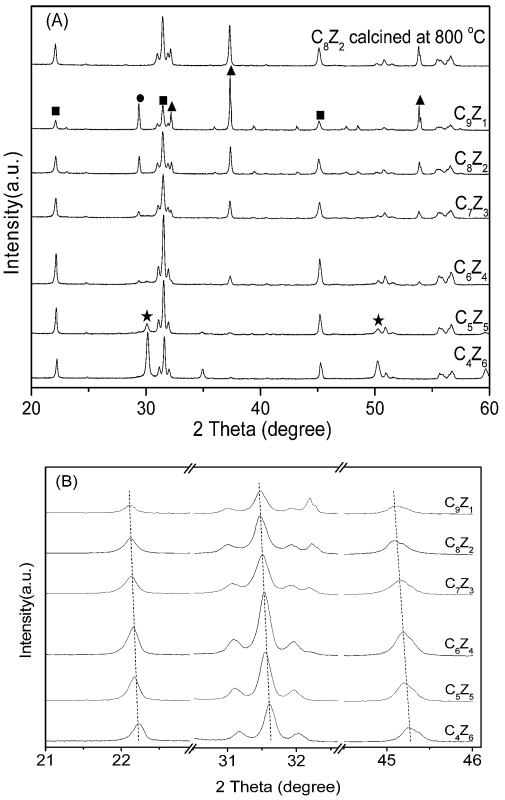

Fig. 2 (A) XRD patterns of the as-prepared $CaO-ZrO_2$ catalysts with different Ca/Zr molar ratio, (B) magnification XRD patterns of the $CaZrO_3$ phase in $CaO-ZrO_2$ catalysts. (▲) CaO; (★) ZrO_2 (tetragonal); (■) $CaZrO_3$; (●) $CaCO_3$.

intensity of $CaZrO_3$ diffraction peaks enhances firstly and then decrease, and a maximum is obtained for the C_6Z_4 sample. This phenomenon can be explained as follows: when Ca/Zr ratio is below 6/4, a portion of ZrO_2 exist in tetragonal zirconia (t-ZrO_2, $2\theta = 30.3°$, 50.2°, JCPDS 88-1007), and it hinders the formation and crystallization of $CaZrO_3$. An analogous depression effect of the free CaO phase on the formation and crystallization of $CaZrO_3$ occurs as the Ca/Zr ratio higher than 6/4. A careful examination of the XRD pattern exhibited in Fig. 2(B) reveals that the diffraction peaks of $CaZrO_3$ shift to lower degree from C_4Z_6 to C_9Z_1. This is because that Zr^{4+} (radius 0.86 Å) in $CaZrO_3$ was substituted by Ca^{2+} cations (radius 0.99 Å) resulting an increase in the crystal lattice parameter.[26] Moreover, as shown in Fig. 2(A), a diffraction peak at 2θ of 29.4° identical to the incompletely decomposed $CaCO_3$, which may be produced during the combustion reaction and/or the air-exposure, is detected for the samples of C_7Z_3, C_8Z_2 and C_9Z_1, and its intensity increase with the increase in Ca/Zr molar ratio.

To estimate the effect of high temperature and longtime calcination procedure on the $CaO-ZrO_2$ structure, the C_8Z_2 sample prepared by combustion method was further calcined at 800 °C for 6 h and examined by XRD. As shown in Fig. 2(A), the diffraction patterns of the as-prepared samples with/without a calcination procedure show no significant differences except the disappearance of a tiny diffraction peak of $CaCO_3$ after calcining. These results indicate that the temperature during the combustion reaction is high enough to promote the synthesis of $CaO-ZrO_2$ in spite of a short reaction time. This is in agreement with the result of TG-DSC. Again, calcining step at a higher temperature only promote the degree of crystallinity and the grain growth.

The BET surface area and the pore volume measured by nitrogen physisorption for $CaO-ZrO_2$ catalysts are presented in Table 1. An increase in the Ca amount leads to a gradual decrease in the BET surface area and the minimum is 1.84 $m^2\ g^{-1}$ for the C_9Z_1 sample. The similar variation was observed for the pore volume of catalysts. This is because that the specific surface area of CaO is much lower than that of ZrO_2;[42] as the Ca/Zr range from 4/6 to 9/1, the independent phase of ZrO_2 vanishes accompanying the appearance of separated CaO phase. Moreover, the decrease in the surface area and pore volume is also related to the partial blocking of the pores in catalysts by CaO.[19,22,43]

Fig. 3 shows the SEM micrograph of the as-prepared C_8Z_2 sample. A cluster of uniform flakes with the thickness less than 0.2 μm was observed. The agglomeration is not significant although the sample suffer from a combustion process with a high temperature of 1000 °C. This can be ascribed to the short duration of combustion and the evolution of a large quantity of gases, which hinder the agglomeration of the $CaO-ZrO_2$ mixed oxide.

3.3. Basicity of the catalysts

The surface base properties of catalysts were investigated by CO_2-TPD technique, and the CO_2 desorption profiles obtained for $CaO-ZrO_2$ with different Ca/Zr molar ratios are presented in Fig. 4. It can be seen that a desorption peak (denoted as α) appears at 450–550 °C for all samples. The intensity of α peak increases first and then decreases with increasing the Ca/Zr ratio, and a maximum is obtained over the C_6Z_4 sample. The α peak is attributed to the interaction of CO_2 with the strong basic sites on the surface of $CaZrO_3$.[26,42] In the temperature range of 520–650 °C, the catalysts with Ca/Zr ratio of ≥6/4 exhibit another desorption peak (denoted as β), and it is related to the stronger basic site of the free CaO aggregated on the surface of the catalysts.[26] Moreover, a negligible desorption

Table 1 BET surface area, pore volume of $CaO-ZrO_2$ catalysts with different Ca/Zr molar ratios and the TOF for FAME formation

Catalyst	S_{BET} ($m^2\ g^{-1}$)	Pore volume ($cm^3\ g^{-1}$)	TOF × 10^{3a} (s^{-1})
C_4Z_6	6.87	0.0145	—[b]
C_5Z_5	3.86	0.0101	36.3
C_6Z_4	2.77	0.0075	49.1
C_7Z_3	2.54	0.0063	49.9
C_8Z_2	2.50	0.0062	55.6
C_9Z_1	1.84	0.0015	42.8

[a] Reaction conditions: catalyst loading = 1.25 wt%, methanol to oil molar ratio = 25 : 1, reaction temperature = 65 °C, reaction time = 1 h. [b] The FAME yield is too low to be detected under the reaction conditions.

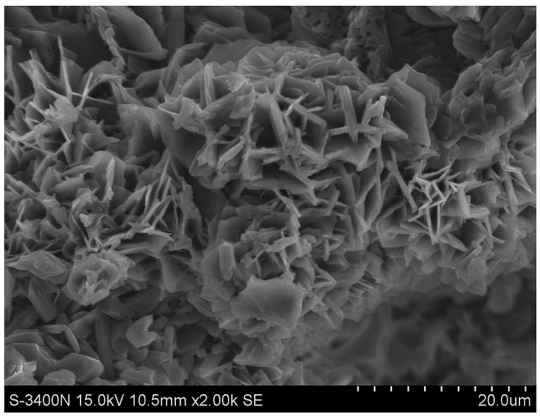

Fig. 3 SEM micrograph of the C_8Z_2 sample.

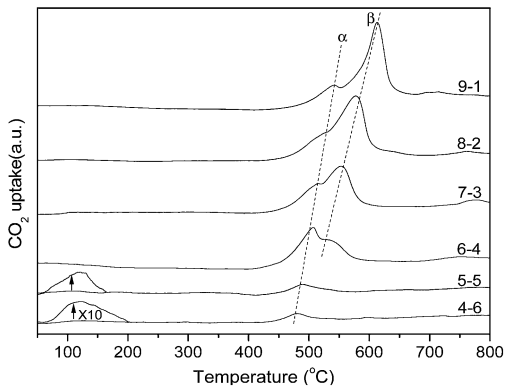

Fig. 4 CO_2-TPD curves of CaO–ZrO_2 catalysts with different Ca/Zr molar ratio.

peak located at 125 °C can be detected only for the samples of C_4Z_6 and C_5Z_5, which corresponds to the surface weak basic site of ZrO_2.[26,44] The results of the CO_2 desorption profiles with various Ca/Zr molar ratio coincide with that of XRD pattern aforementioned. It is noteworthy that with the increase in Ca/Zr molar ratios, α and β peaks shift toward higher temperature, suggesting a continuous increase in the strength of basic sites, and the maximum of peaks are listed in Table 2. As well documented, the strong basicity over the surface of oxide is mainly originated from the isolated (or low coordination) oxygen anions;[34,41,45,46] the greater an oxygen anion's electro-donating is, the stronger its Lewis basicity will be. The results of the XRD had shown that more Zr^{4+} neighboring O^{2-} anion were substituted by Ca^{2+} with increasing the Ca/Zr ratio. Because the electronegativity of Ca^{2+} is smaller than that of Zr^{4+},[26] the electrodonating property of oxygen anions over the surface of $CaZrO_3$ enhance with the increase in Ca/Zr ratio, resulting in the increase in the strength of basic sites and the shift of α peak toward higher temperature. As β peak is concerned, the shift of peak may relate to the interaction between CaO and ZrO_2, which will weaken the basicity of CaO. With the increase in CaO content, more CaO was separated from the mixed oxide and aggregated on the surface, as shown in XRD pattern, accompanying with a decrease in the interaction between CaO and ZrO_2.

Table 2 The maximum temperature of CO_2 desorption and the amount of basic site over Ca–ZrO_2 catalysts with different Ca/Zr molar ratio

Catalyst	T_α (°C)	T_β (°C)	Number of basic sites (mmol g^{-1})		Number of total basic sites (mmol g^{-1})
			Site α	Site β	
C_4Z_6	481	—	0.046	—	0.046
C_5Z_5	490	—	0.083	—	0.083
C_6Z_4	507	531	0.299	0.094	0.393
C_7Z_3	518	553	0.277	0.174	0.451
C_8Z_2	530	577	0.233	0.419	0.652
C_9Z_1	542	613	0.156	0.426	0.582

The number of different base site was evaluated by calculating the integral of each peak, and the data were summarized in Table 2. As shown in Table 2, the number of α basic site takes on a volcanic variation trend with the elevation of Ca/Zr ratio, and a maximum of 0.299 mmol g^{-1} is observed for C_6Z_4. In the case of β basic site, the number increases continuously from C_6Z_4 to C_9Z_1. It should be noted that the amount of CO_2 derived from β peak include the contribution of the decomposition of residual $CaCO_3$, which exists in the catalysts with Ca/Zr ratio above 7/3 (see Fig. 2(A)). Similar results were reported by some authors,[44,47] and they treat the incompletely decomposed $CaCO_3$ as structural carbonate. Furthermore, it can be seen that the total basicity is low for C_4Z_6 and C_5Z_5, and an abrupt increase is observed when the Ca/Zr ratio increase to 6/4, and then the fluctuation of the total basicity slows down. The sequence of total basic sites number is reverse to that of BET surface shown in Table 1. Similar result was reported by Kouzu *et al.* for CaO solid base catalysts.[48]

3.4. Catalytic activity of the catalysts

The FAME yield over CaO–ZrO_2 catalysts with different Ca/Zr ratios as a function of reaction time were presented in Fig. 5. Since the transesterification is a reversible reaction, a high methanol/oil ratio is favorable to shift the equilibrium towards the direction of FAME formation. Moreover, the excess methanol accelerates the remove of product molecules from the catalyst surface and further the regeneration of the active sites.[28] Therefore, a high methanol/oil molar ratio of 25 : 1 was employed in this study, and similar value of methanol/oil ratio could be found in the literature.[21,44,49] It is reported that the mass transfer would be the rate determining step when the catalyst amount is high.[19,49] In order to diminish the influence of mass transfer limitation, a low content of catalyst dosage (1.25 wt% of oil) was used. The reaction was run at 65 °C corresponding to the boiling point of methanol under atmosphere pressure. It can be seen from Fig. 5 that the FAME yield increases rapidly first with the increase in reaction time, and then reaches a steady region. The C_8Z_2 sample exhibits the highest catalytic activity, and the FAME yield of 93.9% and 98%

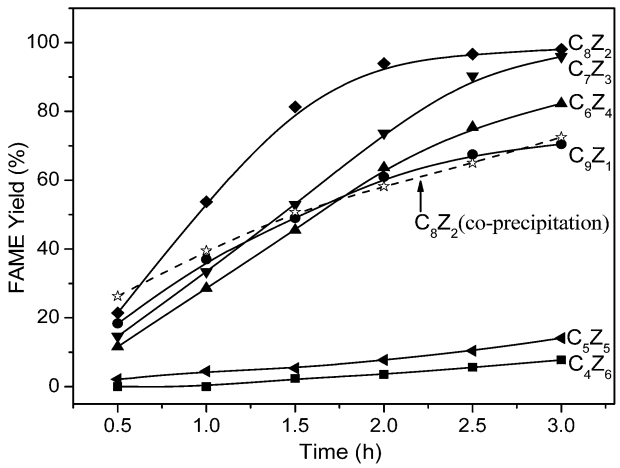

Fig. 5 Effect of reaction time on the FAME yield. Reaction conditions: catalyst loading = 1.25 wt%, methanol to oil molar ratio = 25 : 1, reaction temperature = 65 °C.

were obtained after 2 and 3 h reaction time, respectively. However, the FAME yields over the C_4Z_6 and C_5Z_5 samples are less than 15% even in a reaction time of 3 h. In general, the profile of the FAME yield against the reaction time takes on a shape of sigmoid, and the whole period can be divided into three stages.[13,17,19] At the initial stage, the reaction rate, which depends on the rate of mass transfer of the reactants, is quite low. Then, an abrupt increase in reaction rate appears, and this stage corresponds to the chemical reaction controlled regime. Finally, the reaction becomes slow again at the third stage for the reason of thermodynamic equilibrium. In this study, the absence of the stage of mass transfer limitation may be ascribed to the selection of reaction condition aforementioned.

The catalytic activity over the C_8Z_2 sample prepared by carbonate co-precipitation method was also presented in Fig. 5, for the purpose of comparison. It is obvious that the catalyst prepared by carbonate co-precipitation method is less active for the biodiesel synthesis. For example, after 2 h reaction time, the FAME yield over the C_8Z_2 sample prepared by carbonate co-precipitation is 58.2%, which is far below the value of 93.9% over the counterpart prepared by combustion method. The high-temperature and long-time calcination step was involved during the preparation, which might be responsible for the low FAME yield over the CaO–ZrO_2 catalyst prepared by the co-precipitation method.

To check the possibility of leaching, an experiment was carried out according to the literature.[22] The C_8Z_2 sample prepared by combustion method was placed in contact with methanol under the same conditions as used in the transesterification process, except for the presence of soybean oil. After 3 h of contact, the catalyst was removed by filtration and the recovered methanol was used for transesterification reaction of soybean oil. The reaction was maintained at 65 °C for 3 h, and a FAME yield of about 2% was obtained. This result indicates that the leached active species contributed slightly to the transesterification of soybean oil with methanol.

The studies of mechanism of transesterification reaction illustrate that the role of the basic sites is to abstract proton from organic matter and then develop a series of nucleophile such as methoxide anions, mono-glyceroxide and di-glyceroxide anions, which initiates the transesterification reaction.[3,22,50] Therefore, it is significant to explore the relationship between the catalytic activity and the basicity of the catalysts. The variation of the FAME yield and the total amount of basic sites with the Ca/Zr molar ratio were presented in Fig. 6 together. The value of FAME yield are collected at reaction time of 1.0 h, to ensure that the transesterification reaction are in the chemical reaction controlled regime. Apparently, except for the C_9Z_1 sample, the variation of the FAME yield with the change of Ca/Zr ratio correlates well with that of total amount of basic sites. The deviation of C_9Z_1 can be ascribed to that the evaluations of basic sites for C_9Z_1 by integrating the peak area of CO_2-TPD profile include partial CO_2 originated from the decomposition of structural $CaCO_3$, as mentioned above in CO_2-TPD.

TOF (turnover frequency) of FAME formation (at reaction time of 1.0 h), which represents the molecular number of FAME formed per second per basic site, have been calculated for CaO–ZrO_2 catalysts and the results are listed in Table 1. It can be seen that the values of TOF increase from 36.3 to 55.6 $\times$ 10^{-3} s^{-1} with the Ca/Zr ratio varied from 5/5 to 8/2, which approximate to the values (32.8–85.0 $\times$ 10^{-3} s^{-1}) reported by Song *et al.*[51] Conditioning on that the active sites involved in the rate-determining step are all equally active, the value of TOF should be a constant.[52] As mentioned above, for the transesterification of soybean oil with methanol over CaO–ZrO_2 catalysts, there are two type basic sites (*i.e.* active sites), which results from the isolated (or low coordination) oxygen anion over the surface of $CaZrO_3$ and CaO, respectively. Simultaneously, the results of CO_2-TPD revealed that the strength of the two type basic sites increased continuously with increasing the Ca/Zr ratio. Ding *et al.*[14] reported that the stronger basicity a catalyst had, the higher transesterification activity could be achieved, and the same viewpoint was suggested by Kouzu

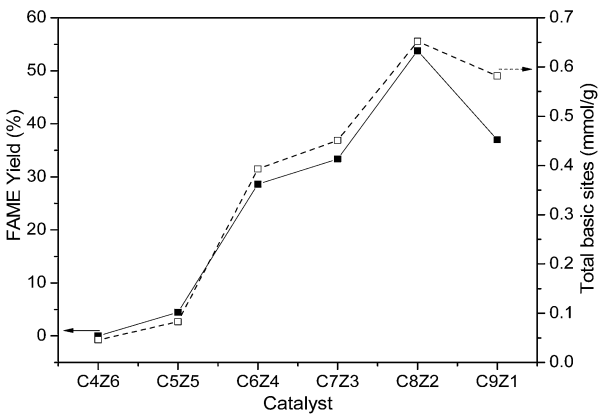

Fig. 6 Effect of Ca/Zr molar ratio on the FAME yield and the total basic sites. Reaction conditions: catalyst loading = 1.25 wt%, methanol to oil molar ratio = 25 : 1, reaction temperature = 65 °C, and reaction time = 1.0 h.

et al.[17] Thereby, the values of TOF increase from C_5Z_5 to C_8Z_2. As for the C_9Z_1 sample, though it possesses the stronger basic site, the value of TOF is lower than that of C_8Z_2, and the reason may also attribute to the error of the evaluation of basic sites. Based on these results, it can be summarized that the catalytic activity are related to both the amount and strength of basic sites.

4. Conclusions

$CaO–ZrO_2$ catalysts with Ca/Zr ratios ranged from 4/6 to 9/1 were prepared *via* urea–nitrate combustion method, and used to catalyze transesterification of soybean oil with methanol for the biodiesel synthesis. The influences of Ca/Zr ratio on the physicochemical and catalytic properties of catalysts were investigated. Based on the results of this work, the following conclusions can be made:

1. The urea–nitrate combustion method was demonstrated to be a simple, fast and effective method for the preparation of $CaO–ZrO_2$ solid base catalysts without a further high temperature and longtime calcination step.

2. The substitution occurs between $Zr^{4+}$and Ca^{2+}, and a new phase of $CaZrO_3$ has been formed for the investigated $CaO–ZrO_2$ catalysts.

3. With the increase in Ca/Zr molar ratio, the BET surface decrease, whereas the total basic sites increase and a maximum is obtained over the C_8Z_2 sample.

4. With the increase in Ca/Zr molar ratio, the strength of the basic site becomes stronger, resulting in a higher turnover frequency (TOF) for transesterification reaction.

5. The sequence of catalytic activity for the synthesis of biodiesel is in agreement with the total basic sites and the catalyst with Ca/Zr ratios of 8/2 exhibits the highest catalytic activity.

Acknowledgements

The authors thank Shanghai Municipal Education Commission (no. 13YZ117), Shanghai Municipal Science and Technology Commission (no. 13ZR1441200) and the National Natural Science Foundation of China (no. 21273150) for financial support.

Notes and references

1 F. Ma and M. A. Hanna, *Bioresour. Technol.*, 1999, **70**, 1.
2 S. A. Basha, K. R. Gopal and S. Jebaraj, *Renewable Sustainable Energy Rev.*, 2009, **13**, 1628.
3 E. Santacesaria, G. M. Vicente, M. Di Serio and R. Tesser, *Catal. Today*, 2012, **195**, 2.
4 Y. Kuwahara, K. Tsuji, T. Ohmichi, T. Kamegawa, K. Mori and H. Yamashita, *Catal. Sci. Technol.*, 2012, **2**, 1842.
5 M. Kim, C. DiMaggio, S. O. Salley and K. Y. Simon Ng, *Bioresour. Technol.*, 2012, **118**, 37.
6 D. E. Lopez, J. G. Goodwin Jr, D. A. Bruce and E. Lotero, *Appl. Catal., A*, 2005, **295**, 97.
7 Y. H. Li, B. Ye, J. W. Shen, Z. Tian, L. J. Wang, L. P. Zhu, T. Ma, D. Y. Yang and F. X. Qiu, *Bioresour. Technol.*, 2013, **137**, 220.
8 J. Tantirungrotechai, S. Thepwatee and B. Yoosuk, *Fuel*, 2013, **106**, 279.
9 A. C. Dimian, Z. W. Srokol, M. C. Mittelmeijer-Hazeleger and G. Rothenberg, *Top. Catal.*, 2010, **53**, 1197.
10 M. L. Grecea, A. C. Dimian, S. Tanase, V. Subbiah and G. Rothenberg, *Catal. Sci. Technol.*, 2012, **2**, 1500.
11 A. A. Kiss, A. C. Dimian and G. Rothenberg, *Energy Fuels*, 2008, **22**, 598.
12 Z. Z. Wen, X. H. Yu, S. T. Tu, J. Y. Yan and E. Dahlquist, *Appl. Energy*, 2010, **87**, 743.
13 V. G. Deshmane and Y. G. Adewuyi, *Fuel*, 2013, **107**, 474.
14 Y. Q. Ding, H. Sun, J. Z. Duan, P. Chen, H. Lou and X. M. Zheng, *Catal. Commun.*, 2011, **12**, 606.
15 M. Kouzu, M. Tsunomori, S. Yamanaka and J. Hidaka, *Adv. Powder Technol.*, 2010, **21**, 488.
16 W. Roschat, M. Kacha, B. Yoosuk, T. Sudyoadsuk and V. Promarak, *Fuel*, 2012, **98**, 194.
17 M. Kouzu and J. S. Hidaka, *Fuel*, 2012, **93**, 1.
18 X. J. Liu, H. Y. He, Y. J. Wang, S. L. Zhu and X. L. Piao, *Fuel*, 2008, **87**, 216.
19 H. T. Wu, J. H. Zhang, Q. Wei, J. L. Zheng and J. A. Zhang, *Fuel Process. Technol.*, 2013, **109**, 13.
20 S. Gryglewicz, *Bioresour. Technol.*, 1999, **70**, 249.
21 L. S. Hsieh, U. Kumar and J. C. S. Wu, *Chem. Eng. J.*, 2010, **158**, 250.
22 N. Pasupulety, K. Gunda, Y. Q. Liu, G. L. Rempel and F. T. T. Ng, *Appl. Catal., A*, 2013, **452**, 189.
23 Y. L. Meng, B. Y. Wang, S. F. Li, S. J. Tian and M. H. Zhang, *Bioresour. Technol.*, 2013, **128**, 305.
24 H. Sun, J. Z. Duan, P. Chen, H. Lou and X. M. Zheng, *Catal. Commun.*, 2011, **12**, 1005.
25 A. M. Dehkordi and M. Ghasemi, *Fuel Process. Technol.*, 2012, **97**, 45.
26 H. Wang, M. H. Wang, S. G. Liu, N. Zhao, W. Wei and Y. H. Sun, *J. Mol. Catal. A: Chem.*, 2006, **258**, 308.
27 H. Wang, S. G. Liu, W. Y. Zhang, N. Zhao, W. Wei and Y. H. Sun, *Acta Chim. Sin.*, 2006, **64**, 2409.
28 N. Kaur and A. Ali, *Fuel Process. Technol.*, 2014, **119**, 173.
29 J. B. Chen, J. W. Su, J. M. Qi, X. X. Chen and L. Chen, *Chin. J. Appl. Chem.*, 2011, **28**, 267.
30 K. C. Patil, S. T. Aruna and T. Mimani, *Curr. Opin. Solid State Mater. Sci.*, 2002, **6**, 507.
31 J. Papavasiliou, G. Avgouropoulos and T. Ioannides, *Appl. Catal., B*, 2006, **66**, 168.
32 X. M. Guo, D. S. Mao, S. Wang, G. S. Wu and G. Z. Lu, *Catal. Commun.*, 2009, **10**, 1661.
33 X. M. Guo, D. S. Mao, G. Z. Lu, S. Wang and G. S. Wu, *J. Catal.*, 2010, **271**, 178.
34 G. Gelbard, O. Bres, R. M. Vargas, F. Vielfaure and U. F. Schuchardt, *J. Am. Oil Chem. Soc.*, 1995, **72**, 1239.
35 R. D. Purohit, B. P. Sharma, K. T. Pillai and A. K. Tyagi, *Mater. Res. Bull.*, 2001, **36**, 2711.
36 M. J. de Andrade, M. D. Lima, R. Bonadiman and C. P. Bergmann, *Mater. Res. Bull.*, 2006, **41**, 2070.
37 S. R. Jain, K. C. Adiga and V. R. Pai Verneker, *Combust. Flame*, 1981, **40**, 71.

38 D. A. Fumo, M. R. Morelli and A. M. Segadães, *Mater. Res. Bull.*, 1996, **31**, 1243.
39 J. C. Toniolo, M. D. Lima, A. S. Takimi and C. P. Bergmann, *Mater. Res. Bull.*, 2005, **40**, 561.
40 C. Liu, P. M. Lv, Z. H. Yuan, F. Yan and W. Luo, *Renewable Energy*, 2010, **35**, 1531.
41 W. N. N. W. Omar and N. A. S. Amin, *Fuel Process. Technol.*, 2011, **92**, 2397.
42 H. Wang, M. H. Wang, W. Y. Zhang, N. Zhao, W. Wei and Y. H. Sun, *Catal. Today*, 2006, **115**, 107.
43 Y. H. T. Yap, H. V. Lee, R. Yunus and J. C. Juan, *Chem. Eng. J.*, 2011, **178**, 342.
44 H. Sun, Y. Q. Ding, J. Z. Duan, Q. J. Zhang, Z. Y. Wang, H. Lou and X. M. Zheng, *Bioresour. Technol.*, 2010, **101**, 953.
45 M. Verziu, B. Cojocaru, J. Hu, R. Richards, C. Ciuculescu, P. Filip and V. I. Parvulescu, *Green Chem.*, 2008, **10**, 373.
46 V. K. Díez, C. R. Apesteguía and J. I. Dí Cosimo, *Catal. Today*, 2000, **63**, 53.
47 S. Sato, R. Takahashi, M. Kobune and H. Gotoh, *Appl. Catal., A*, 2009, **356**, 57.
48 M. Kouzu, T. Kasuno, M. Tajika, Y. Sugimoto, S. Yamanaka and J. Hidaka, *Fuel*, 2008, **87**, 2798.
49 X. J. Liu, X. L. Piao, Y. J. Wang, S. L. Zhu and H. Y. He, *Fuel*, 2008, **87**, 1076.
50 M. Kouzu, T. Kasuno, M. Tajika, S. Yamanaka and J. Hidaka, *Appl. Catal., A*, 2008, **334**, 357.
51 R. L. Song, D. M. Tong, J. Q. Tang and C. W. Hu, *Energy Fuels*, 2011, **25**, 2679.
52 M. Boudart, *Chem. Rev.*, 1995, **95**, 661.